We are IntechOpen,
the world's leading publisher of
Open Access books
Built by scientists, for scientists

6,900
Open access books available

185,000
International authors and editors

200M
Downloads

Our authors are among the

154
Countries delivered to

TOP 1%
most cited scientists

12.2%
Contributors from top 500 universities

CLARIVATE ANALYTICS

BOOK
CITATION
INDEX

INDEXED

WEB OF SCIENCE™

Selection of our books indexed in the Book Citation Index
in Web of Science™ Core Collection (BKCI)

Interested in publishing with us?
Contact book.department@intechopen.com

Numbers displayed above are based on latest data collected.
For more information visit www.intechopen.com

2

Direction-Selective Filters for Sound Localization

Dean Schmidlin
El Roi Analytical Services
United States of America

1. Introduction

An important problem in sound localization is the determination of the polar and azimuthal angles of far-field acoustic sources. Two fundamental approaches to the solution can be identified: spatial filtering (beamforming) and the parameter estimation approach. Van Veen and Buckley (1988) and Krim and Viberg (1996) give comprehensive reviews of the first and second approaches, respectively. Spatial filtering was carried out by an array of pressure sensors. A serious drawback to the filtering approach is that its performance depends directly on the physical size of the array (aperture), regardless of the data gathering time and signal-to-noise ratio. This aperture dependence together with more demanding applications motivated a good number of researchers to develop parametric estimation techniques. These methods can be separated into two main categories, namely, spectral-based and parametric approaches. The most famous example of the first is MUSIC (MUltiple Signal Classification) algorithm developed by Schmidt (1981) and Bienvenu and Kopp (1980), and of the second is the Maximum Likelihood (ML) method developed by Kumaresan and Shaw (1985) and Bresler and Macovski (1986).

In contrast to beamforming techniques, a MUSIC estimate of arbitrary accuracy can be achieved if the data gathering time is sufficiently long, the SNR high enough, and the signal model sufficiently accurate. However, a significant limitation is the inability to resolve closely spaced signals with small sample sizes and low SNR. Further deterioration occurs for highly correlated signals and complete breakdown for coherent signals. The interested reader is referred to Krim and Viberg (1996) for discussions on how these limitations have been addressed.

All of the methods for localizing acoustic sources had one thing in common. They used arrays composed of pressure sensors. This continued until Nehorai and Paldi (1994) introduced a new type of sensor called the vector sensor. An acoustic vector sensor measures the acoustic pressure and all three components of the acoustic particle velocity at a single point in space. The extra information provided by the vector sensor opened the door to improved source localization accuracy without increase in array aperture. Vector-sensor models and fundamental processing techniques were developed by Nehorai and Paldi (1994) and Hawkes and Nehorai (2000) for the case of sensors located away from and in the presence of a reflecting boundary, respectively. Parametric techniques that had been designed for arrays of pressure sensors were adapted to vector sensors. For example, Wong

and Zoltowski (1999), (2000) introduced Root-MUSIC-based and MUSIC-based source localization algorithms for vector sensors. Theoretical and technological development of the vector sensor also revitalized interest in using spatial filtering (beamforming) to localize acoustic sound sources (D'Spain *et al.*, 1992; Hawkes and Nehorai, 1998; Wong and Chi, 2002; Zou and Nehorai, 2009).

D'Spain et al. (2006) pointed out that the Taylor series expansion of the acoustic pressure field about a single point in space provides the theoretical basis for array processing with measurements at a single point in space. Since the particle velocity is proportional to the gradient of the pressure, the vector sensor provides information for the first two terms in the Taylor series. Silvia et al. (2001) used the Taylor series to define a general class of directional acoustic receivers based on the number of series terms measured by the receiver. Based on this definition, a pressure sensor is considered as a directional acoustic sensor of order zero, and a vector sensor is referred to as a directional acoustic sensor of order one. Silvia (2001) performed a theoretical and experimental investigation of an acoustic sensor of order two. It was given the name "dyadic sensor" because in addition to measuring the pressure and the gradient of the pressure, it also measures the dyadic of the pressure. Cray (2002) and Cray *et al.* (2003) presented theory for acoustic receivers of order greater than two. Schmidlin (2007) extended the multichannel filtering approach of Silvia (2001) to directional acoustic sensors of arbitrary order ν. It was shown that the maximum directivity index is $20\log(1+\nu)$, and explicit expressions were derived for the optimum weights.

The primary interest in "beamforming from a single point in space" is the achievement of high directivity with a sensor system occupying a smaller area of space than the conventional pressure array. However, it is very difficult to physically measure the higher–order spatial partial derivatives of the pressure. This led to indirect means for measuring these derivatives. Hines *et al.* (2000) used the method of finite differences to implement a superdirective line array and Schmidlin (2010a) introduced a distribution theory approach for implementing directional acoustic sensors. Another difficulty with highly directional receivers is sensitivity to uncorrelated system noise (Hines and Hutt, 1999; Hines *et al.*, 2000; Cray, 2001). System noise includes pre-amplifier voltage noise, inter-channel imbalance in gain and/or phase, sensor spacing errors, acoustic scatter and hydrophone self-noise due to hydrodynamic flow past the sensors.

In the theory of digital filters, causal FIR filters and IIR filters have transfer functions that are polynomial functions and rational functions, respectively, of the complex variable z^{-1}. The primary advantage of IIR filters over FIR filters is that they usually satisfy a particular set of specifications with a much lower filter order than a corresponding order FIR filter. This paper uses this advantage as the starting point for generating direction-selective filters. Directional acoustic sensors have beampatterns that are polynomial functions of the direction cosine $\cos\psi$. The direction-selective filters presented herein have beampatterns that are rational functions of $\cos\psi$. Section 2 analyzes a first-order filter prototype, develops the concept of a discriminating function, and derives an expression for its directivity index. In Section 3, prototypical filters are connected in parallel to realize rational discriminating functions, and a detailed example is presented. It is also shown that a discriminating function can be designed from the magnitude-squared response of a digital filter. Section 4 summarizes the contents of the paper and discusses future research.

2. Direction-selective filters tuned to the look direction

2.1 Vector sensor as a direction-selective filter

A plane wave is traveling towards the origin of a rectangular coordinate system. Located at the origin is a directional acoustic sensor. If this sensor is a vector sensor then the expression for the linear beamformer output for the look direction u_L is given by (D'Spain *et al.*, 2006)

$$p_o(t) = a_0 p(t) + \rho_0 c \sum_{j=1}^{3} a_j \left[\upsilon_j(t) + n_j(t) \right] \cos \beta_j \tag{1}$$

The components of the look direction are the direction cosines $\cos \beta_j, j = 1, 2, 3$ where

$$\begin{aligned} \cos \beta_1 &= \cos \theta_L \sin \phi_L \\ \cos \beta_2 &= \sin \theta_L \sin \phi_L \\ \cos \beta_3 &= \cos \phi_L \end{aligned} \tag{2}$$

where the angles θ_L is the azimuthal angle and ϕ_L the polar or zenith angle. The time function $p(t)$ is the acoustic pressure at the origin and $\upsilon_j(t), j = 1, 2, 3$ the three orthogonal components of the acoustic particle velocity. The function $n_j(t)$ represents the self-noise at the $j-$th velocity sensor and $\rho_0 c$ the characteristic impedance of the medium. Ignoring the self-noise at each velocity sensor and letting $a_j = -a_\upsilon$ for $j = 1, 2, 3$ simplifies Eq. (1) to

$$p_o(t) = a_0 p(t) - \rho_0 c a_\upsilon \mathbf{v}(t) \cdot u_L \tag{3}$$

The particle velocity at time t and position r is related to the pressure as follows (Ziomek, 1995)

$$\mathbf{v}(t, r) = -\frac{p(t + u \cdot r/c)}{\rho_0 c} u \tag{4}$$

Setting r to 0 and placing the result into Eq. (3) results in

$$p_o(t) = (a_0 + a_\upsilon u \cdot u_L) p(t) \tag{5}$$

The unit-vector u points in the direction of the arriving plane wave and the unit-vector u_L points in the look direction. The scalar product $u \cdot u_L$ is equal to the cosine of the angle ψ between them. If

$$g_{u_L}(\psi) \equiv a_0 + a_\upsilon u \cdot u_L = a_0 + a_\upsilon \cos \psi \tag{6}$$

then the output of the linear beamformer is expressed as

$$p_o(t) = g_{u_L}(\psi) p(t) \tag{7}$$

The function $g_{u_L}(\psi)$ has some selectivity with regards to the direction of the plane wave and is generally referred to as the beampattern of the vector sensor. If the pair of weights are given the assignments

$$a_0 = -\frac{b}{1-b}, a_\nu = \frac{1}{1-b} \tag{8}$$

then

$$g_{u_L}(\psi) = \frac{\cos\psi - b}{1-b} \tag{9}$$

The angle ψ goes from 0 to π. When $\psi = 0$, the plane wave is arriving in the look direction and $g_{u_L}(0) = 1$. When $\psi = \pi$, the plane wave is arriving in a direction opposite to the look direction and

$$g_{u_L}(\pi) = -\frac{1+b}{1-b} \tag{10}$$

Since it is desired that $\left|g_{u_L}(\pi)\right| < \left|g_{u_L}(0)\right| = 1$, the value of b must be negative. If the magnitude of b is not greater than 1, then $g_{u_L}(\psi) = 0$ at $\psi = \cos^{-1} b$ and the vector sensor will have nulls. It has been shown by the author (2010b) that the null directions are given by

$$u = (u_1 \cos\zeta + u_2 \sin\zeta)\sqrt{1-b^2} + b u_L \tag{11}$$

where $0 \leq \zeta < 2\pi$ and

$$u_L = \begin{bmatrix} \cos\theta_L \sin\phi_L \\ \sin\theta_L \sin\phi_L \\ \cos\phi_L \end{bmatrix} \tag{12}$$

$$u_1 = \begin{bmatrix} \cos\theta_L \cos\phi_L \\ \sin\theta_L \cos\phi_L \\ -\sin\phi_L \end{bmatrix}, u_2 = \begin{bmatrix} -\sin\theta_L \\ \cos\theta_L \\ 0 \end{bmatrix} \tag{13}$$

The unit-vectors u_1, u_2, u_L define the coordinate axes of a new rectangular coordinate system where u_L points in direction of the new z axis. The angles ψ and ζ are the polar and azimuthal angles, respectively. This new coordinate system was generated by making two positive coordinate frame rotations, the first a rotation through an angle θ_L about the original z axis and the second a rotation through an angle ϕ_L about the newly formed y axis. The maximum directivity index occurs at $b = -1/3$ and has the value 6.02 dB.

The input-output equation (7) together with Eq. (9) define a spatial filter. The filter is centered in the direction u_L. In this paper, the function $g_{u_L}(\psi)$ will be called the discriminating function because it favors a plane wave traveling in the look direction while tending to discriminate against plane waves moving in other directions. The discriminating function is a function of only one variable, ψ. If the angle between a direction u of a plane wave and the look direction u_L is ψ_1, then the set of all u vectors that experience the same attenuation $g_{u_L}(\psi_1)$ is specified by

$$u = (u_1 \cos\zeta + u_2 \sin\zeta)\sin\psi_1 + u_L \cos\psi_1 \qquad 0 \leq \zeta < 2\pi \tag{14}$$

Equation (14) follows from Eq. (11). Note that when $\psi_1 = 0$, $\mathrm{u} = \mathrm{u}_L$ and when $\psi_1 = \pi$, $\mathrm{u} = -\mathrm{u}_L$. Both cases consist of only a single vector in the set.

In the Introduction it was mentioned that the vector sensor is called a directional acoustic sensor of order one. It owes its filtering capability to the fact that its discriminating function contains the scalar product $\mathrm{u} \cdot \mathrm{u}_L$. One can extend the order of the directional acoustic sensor by beginning with the expression for the acoustic pressure at time t and position r, namely,

$$p(t,\mathrm{r}) = p\left(t + \frac{\mathrm{u} \cdot \mathrm{r}}{c}\right) \tag{15}$$

Setting r to $r\mathrm{u}_L$ in Eq. (15) yields

$$p(t,r) = p\left(t + \frac{\mathrm{u} \cdot \mathrm{u}_L}{c} r\right) \tag{16}$$

The pressure function was transformed from a four-dimensional function to a two-dimensional one by restricting the spatial points to lie on the radial line extending out from the origin in the look direction u_L. Consider next the two-dimensional integro-differential operator

$$\mathrm{L}[p(t,r)] \equiv c\int \frac{\partial p(t,r)}{\partial r} dt \tag{17}$$

The substitution of Eq. (16) into Eq. (17) results in

$$\mathrm{L}[p(t,r)] \equiv (\mathrm{u} \cdot \mathrm{u}_L)p(t,r) \tag{18}$$

The function $p(t,r)$ is an eigenfunction of the linear operator L and $\mathrm{u} \cdot \mathrm{u}_L$ the associated eigenvalue. A generalized directional acoustic sensor of order v can be defined as one whose beamformer output is given by

$$p_\mathrm{o}(t) = \sum_{n=0}^{v} a_n \mathrm{L}^n[p(t,r)] = g_{\mathrm{u}_L}(\psi)p(t,r) \tag{19}$$

$$g_{\mathrm{u}_L}(\psi) = \sum_{n=0}^{v} a_n \cos^n \psi \tag{20}$$

The discriminating function is a polynomial in $\cos\psi$ of degree v. The optimum directivity index is $20\log(1+v)$ (Schmidlin, 2007). It is a very difficult matter to implement the operations $\mathrm{L}^n[p(t,r)]$ for $n \geq 2$. This accounts for the sparsity of work on higher-order directional acoustic receivers. This paper attempts to alleviate this problem by introducing a special type of spatial filter, one whose discriminating function is a rational function of $\cos\psi$. The prototype filter is presented in the next section.

2.2 First-order prototype filter
The temporal-spatial filter that is to serve as the prototype for the filters considered herein is represented by the linear first-order partial differential equation

$$a\frac{\partial p_{\mathrm{o}}(t,\tau)}{\partial t} - \frac{\partial p_{\mathrm{o}}(t,\tau)}{\partial \tau} + \gamma\, p_{\mathrm{o}}(t,\tau) = K\, p(t,\tau) \tag{21}$$

The variable τ is equal to r/c. The general solution to Eq. (21) when the forcing function is equal to zero is given by (Kythe et al., 2003)

$$p_{\mathrm{o}}(t,\tau) = f(t+a\tau)\exp(-\gamma t/a) \tag{22}$$

The function $f(\cdot)$ is arbitrary. The forcing function of interest is the harmonic plane wave function

$$p(t,\tau) = \exp(j\omega t)\exp(j\omega\tau\cos\psi) \tag{23}$$

The response to this input can be found by assuming a solution of the form

$$p_{\mathrm{o}}(t,\tau) = B(\omega:\psi)\exp(j\omega t)\exp(j\omega\tau\cos\psi) \tag{24}$$

The substitution of Eqs. (23) and (24) into Eq. (21) results in

$$B(\omega:\psi) = \frac{K}{\gamma + j\omega(a-\cos\psi)} \tag{25}$$

The function $B(\omega:\psi)$ is called the beam pattern of the filter. The total solution of the partial differential equation is the sum of the functions of Eqs. (22) and (24). The total solution is made unique by introducing the initial condition $p_{\mathrm{o}}(0,\tau) = 0$. This creates the constraint

$$f(a\tau) + B(\omega:\psi)\exp(j\omega\tau\cos\psi) = 0 \tag{26}$$

Solving for $f(\tau)$ and then $f(t+a\tau)$ gives

$$\begin{aligned} f(\tau) &= -B(\omega:\psi)\exp(j\omega\tau\cos\psi/a) \\ f(t+a\tau) &= -B(\omega:\psi)\exp(j\omega t\cos\psi/a)\exp(j\omega\tau\cos\psi) \end{aligned} \tag{27}$$

The output of the prototype filter in response to the harmonic plane wave input is

$$p_{\mathrm{o}}(t,\tau) = B(\omega:\psi)\exp(j\omega\tau\cos\psi)\big[\exp(j\omega t) - \exp(-\gamma t/a)\exp(j\omega t\cos\psi/a)\big] \tag{28}$$

When $\gamma \neq 0$, the second component within the brackets of Eq. (28) decays to zero as time increases. One observes from Eq. (25) that the beam pattern's sensitivity to variations in the angle ψ decreases with increasing γ. Consequently, a very small γ is desirable. For the special case $\gamma = 0$, Eq. (25) becomes

$$B(\omega:\psi) = \frac{g_{\mathrm{u}_L}(\psi)}{j\omega} \tag{29}$$

$$g_{\mathrm{u}_L}(\psi) = \frac{K}{a-\cos\psi} \tag{30}$$

The function $g_{u_L}(\psi)$ is the discriminating function of the prototype filter. If K is chosen to be $a-1$ then

$$g_{u_L}(0) = 1, \ g_{u_L}(\pi) = \frac{a-1}{a+1} \tag{31}$$

Since it is desirable for the discriminating function at $\psi = \pi$ to be less than one in magnitude, the value of a must be positive. And Eq. (30) reveals that for the discriminating function to be finite for $0 \le \psi \le \pi$, the value of a must be greater than 1. For $\gamma = 0$, the output $p_o(t,\tau)$ becomes

$$p_o(t,\tau) = g_{u_L}(\psi) \frac{\exp(j\omega\tau\cos\psi)}{j\omega} \left[\exp(j\omega t) - \exp(j\omega t\cos\psi/a) \right] \tag{32}$$

Of special interest is the behavior of the filter towards a plane wave coming from the look direction ($\psi = 0$). Equation (32) simplifies to

$$p_o(t,\tau) = \frac{\exp(j\omega\tau)}{j\omega} \left[\exp(j\omega t) - \exp\left(j\frac{\omega}{a}t \right) \right] \tag{33}$$

The output of the prototype filter contains two sinusoidal components. The frequency of the first component is equal to the input frequency ω. The frequency of the second component is equal to ω/a which is less than the input frequency since $a > 1$. This frequency can be eliminated by a temporal bandpass filter. If ω_{min} and ω_{max} denote the minimum and maximum frequencies of interest, then a constraint on the parameter a is

$$\frac{\omega_{max}}{a} < \omega_{min} \Rightarrow a > \frac{\omega_{max}}{\omega_{min}} \tag{34}$$

2.3 Directivity index of prototype filter

In a receiving aperture, directivity serves to reject noise and other interference arriving from directions other than the look direction. The directive effect of a spatial filter has been summarized in a single number called the directivity, which is computed from (Ziomek, 1995)

$$D = \frac{P(\omega:0)}{\frac{1}{4\pi} \int_0^{2\pi} \int_0^{\pi} P(\omega:\psi)\sin\psi \, d\psi \, d\zeta} \tag{35}$$

where $P(\omega:\psi)$ is the filter's beam power pattern and for $\gamma = 0$ is given by

$$P(\omega:\psi) = |B(\omega:\psi)|^2 = \frac{(a-1)^2}{\omega^2(a-\cos\psi)^2} \tag{36}$$

Equation (35) can be simplified to

$$D = \frac{2P(\omega:0)}{\int_{-1}^{1} P(\omega:x)\,dx} \tag{37}$$

where $x = \cos\psi$. The substitution of Eq. (36) into Eq. (37) results in

$$D = \frac{2}{\int_{-1}^{1} \frac{(a-1)^2}{(a-x)^2}\,dx} = \frac{a+1}{a-1} \tag{38}$$

Equation (38) represents the directivity of the first-order prototype filter. The directivity index is defined as

$$\mathrm{DI} \triangleq 10\log_{10} D \text{ dB} \tag{39}$$

Equation (34) gives a constraint on the parameter a. Let $\omega_1 \le \omega_{\min}$ and $\omega_2 \ge \omega_{\max}$ denote the lower and upper cutoff frequencies of the temporal bandpass filter that is to filter out the undesirable frequency component in Eq. (33), and let $a = \omega_2/\omega_1$. The lower and upper cutoff frequencies are related to the center frequency ω_0 and the quality factor Q by

$$\begin{aligned} \omega_1 &= \omega_0\left(\sqrt{1 + \frac{1}{4Q^2}} - \frac{1}{2Q}\right) \\ \omega_2 &= \omega_0\left(\sqrt{1 + \frac{1}{4Q^2}} + \frac{1}{2Q}\right) \end{aligned} \tag{40}$$

From Eq. (40) one may write

$$\frac{\omega_2 + \omega_1}{\omega_2 - \omega_1} = \frac{a+1}{a-1} = \sqrt{1 + 4Q^2} \tag{41}$$

From Eqs. (38) and (39) the directivity index becomes

$$\mathrm{DI} = 10\log_{10}\sqrt{1 + 4Q^2} \tag{42}$$

For $Q \gg 1/2$ the DI may be approximated as

$$\mathrm{DI} = 3 + 10\log_{10} Q \text{ dB} \tag{43}$$

If the input plane wave function fits within the pass band of the temporal filter, then the directivity index is given by Eq. (43). For $Q = 10$, the directivity index is 13 dB. It was noted in Section 2.1 that the maximum directivity index for a vector sensor is 6.02 dB. Using Eq. (41) to Solve for a yields

$$a = \frac{\sqrt{1 + 4Q^2} + 1}{\sqrt{1 + 4Q^2} - 1} \tag{44}$$

When the quality factor is 10, then the parameter a of the prototype filter is 1.105. The discriminating function of the filter is given by Eq. (30). The function has a value of 1 at $\psi = 0$. The beamwidth of the prototype filter is obtained by equating Eq. (30) to $1/\sqrt{2}$, solving for ψ, and multiplying by 2. The result is

$$\mathrm{BW} = 2\psi_{3dB} = 2\cos^{-1}\left[a\left(1-\sqrt{2}\right)+\sqrt{2}\right] \qquad (45)$$

For the case $a = 1.105$, the beamwidth is 33.9°. This is in sharp contrast to the beamwidth of the maximum DI vector sensor which is 104.9°. Figure 1 gives a plot of the discriminating function as a function of the angle ψ. Note that the discriminating function is a monotonic function of ψ. This is not true for discriminating functions of directional acoustic sensors (Schmidlin, 2007).
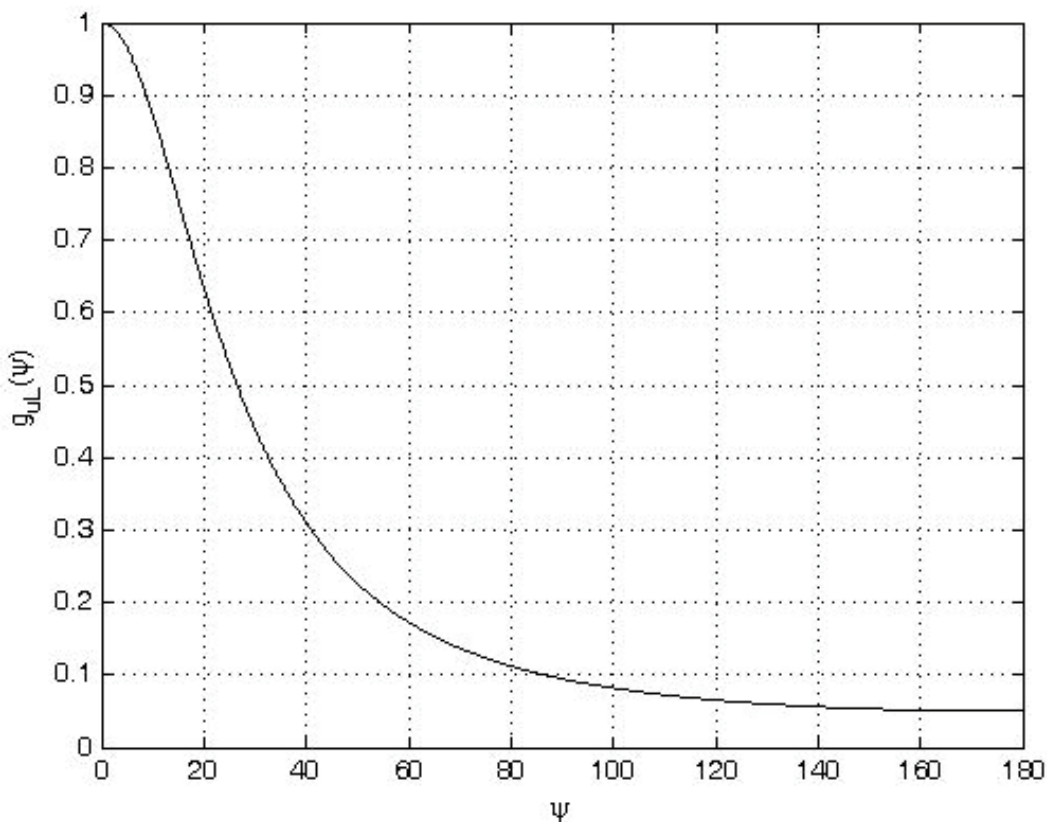

Fig. 1. Discriminating function for $a = 1.105$.

3. Direction-Selective filters with rational discriminating functions

3.1 Interconnection of prototype filters
The first-order prototype filter can be used as a fundamental building block for generating filters that have discriminating functions which are rational functions of $\cos\psi$. As an example, consider a discriminating function that is a proper rational function and whose denominator polynomial has roots that are real and distinct. Such a discriminating function may be expressed as

$$g_{u_L}(\psi) = \frac{\sum\limits_{j=0}^{\mu} d_j \cos^j \psi}{\sum\limits_{j=0}^{\nu} c_j \cos^j \psi} = K \frac{\prod\limits_{j=1}^{\mu}(b_j - \cos\psi)}{\prod\limits_{j=1}^{\nu}(a_j - \cos\psi)} \qquad (46)$$

where $c_\nu = 1$ and $\mu < \nu$. The discriminating function of Eq. (46) can expanded in the partial fraction expansion

$$g_{u_L}(\psi) = \sum\limits_{i=1}^{\nu} \frac{K_i}{a_i - \cos\psi} \qquad (47)$$

The function specified by Eq. (47) may be realized by a parallel interconnection of ν prototype filters (with γ = 0). Each component of the above expansion has the form of Eq. (30). Normalizing the discriminating function such that it has a value of 1 at $\psi = 0$ yields

$$\sum\limits_{i=1}^{\nu} \frac{K_i}{a_i - 1} = 1 \qquad (48)$$

Similar to Eq. (36), the beam power pattern of the composite filter is given by

$$P(\omega : \psi) = \frac{\left| g_{u_L}(\psi) \right|^2}{\omega^2} \qquad (49)$$

Equations (47) and (49) together with Eq. (35) lead to the following expression for the directivity:

$$D^{-1} = \sum\limits_{i=1}^{\nu} \sum\limits_{j=1}^{\nu} K_i K_j g_{ij} \qquad (50)$$

where

$$g_{ii} = \frac{1}{a_i^2 - 1} \qquad (51)$$

$$g_{ij} = \frac{1}{a_i - a_j} \coth^{-1} \left(\frac{a_i a_j - 1}{a_i - a_j} \right), i \neq j \qquad (52)$$

For a given set of a_i values, the directivity can be maximized by minimizing the quadratic form given by Eq. (50) subject to the linear constraint specified by Eq. (48). To solve this optimization problem, it is useful to represent the problem in matrix form, namely,

$$\begin{aligned} &\text{minimize } D^{-1} = \text{K}'\text{GK} \\ &\text{subject to } \text{U}'\text{K} = 1 \end{aligned} \qquad (53)$$

where

$$\mathbf{K'} = \begin{bmatrix} K_1 & K_2 & \cdots & K_v \end{bmatrix} \tag{54}$$

$$\mathbf{U'} = \begin{bmatrix} \dfrac{1}{a_1 - 1} & \dfrac{1}{a_2 - 1} & \cdots & \dfrac{1}{a_v - 1} \end{bmatrix} \tag{55}$$

and *G* is the matrix containing the elements g_{ij}. Utilizing the Method of Lagrange Multipliers, the solution for K is given by

$$\mathbf{K} = \dfrac{\mathbf{G}^{-1}\mathbf{U}}{\mathbf{U'}\mathbf{G}^{-1}\mathbf{U}} \tag{56}$$

The minimum of D^{-1} has the value

$$D^{-1} = \mathbf{U'}\mathbf{G}^{-1}\mathbf{U} \tag{57}$$

The maximum value of the directivity index is

$$\mathrm{DI}_{\max} = -10\log_{10}\left(\mathbf{U'}\mathbf{G}^{-1}\mathbf{U}\right) \tag{58}$$

3.2 An example: a second-degree rational discriminating function

As a example of applying the contents of the previous section, consider the proper rational function of the second degree,

$$g_{\mathrm{u}_L}(\psi) = \dfrac{d_0 + d_1\cos\psi}{c_0 + c_1\cos\psi + \cos^2\psi} = \dfrac{K_1}{a_1 - \cos\psi} + \dfrac{K_2}{a_2 - \cos\psi} \tag{59}$$

where $a_2 > a_1$ and

$$\begin{aligned} d_0 &= a_2 K_1 + a_1 K_2 \\ d_1 &= -K_1 - K_2 \\ c_0 = a_1 a_2, \quad c_1 &= -a_1 - a_2 \end{aligned} \tag{60}$$

In the example presented in Section 2.3, the parameter *a* had the value 1.105. In this example let $a_1 = 1.105$, and let $a_2 = 1.200$. The value of the matrices *G* and *U* are given by

$$\mathbf{G} = \begin{bmatrix} 4.5244 & 3.1590 \\ 3.1590 & 2.227 \end{bmatrix} \tag{61}$$

$$\mathbf{U} = \begin{bmatrix} 9.5238 \\ 5.0000 \end{bmatrix} \tag{62}$$

If Eqs. (56) and (58) are used to compute *K* and $\mathrm{DI}_{\max}$, the result is

$$\mathbf{K} = \begin{bmatrix} 0.3181 \\ -0.4058 \end{bmatrix} \tag{63}$$

$$\mathrm{DI}_{max} = 17.8289 \text{ dB} \tag{64}$$

From Eqs. (60), one obtains

$$d_0 = -.0668, \quad d_1 = 0.0878$$
$$c_0 = 1.3260, \quad c_1 = -2.3050 \tag{65}$$

Figure 2 illustrates the discriminating function specified by Eqs. (59) and (65). Also shown (as a dashed line) for comparison the discriminating function of Fig. 1. The dashed-line plot represents a discriminating function that is a rational function of degree one, whereas the solid-line plot corresponds to a discriminating function that is a rational function of degree two. The latter function decays more quickly having a 3-dB down beamwidth of 22.6° as compared to a 3-dB down beamwidth of 33.9° for the former function.
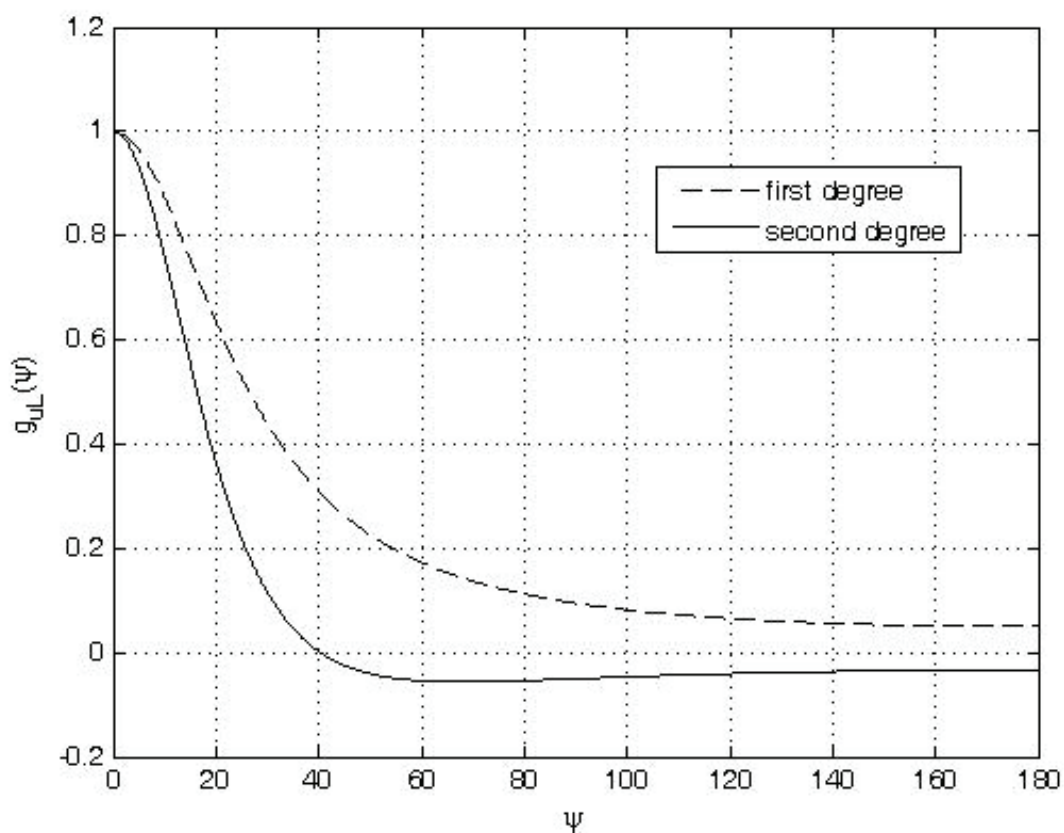

Fig. 2. Plots of the discriminating function of the examples presented in Sections 2.3 and 3.2.

In order to see what directivity index is achievable with a second-degree discriminating function, it is useful to consider the second-degree discriminating function of Eq. (59) with equal roots in the denominator, that is, $c_0 = a^2, c_1 = -2a$. It is shown in a technical report by the author (2010c) that the maximum directivity index for this discriminating function is equal to

$$D_{max} = 4\frac{a+1}{a-1} \tag{66}$$

and is achieved when d_0 and d_1 have the values

$$d_0 = \frac{a-1}{4}(a-3) \tag{67}$$

$$d_1 = \frac{a-1}{4}(3a-1) \tag{68}$$

Note that the directivity given by Eq. (66) is four times the directivity given by Eq. (38). Analogous to Eqs. (42) and (43), the maximum directivity index can be expressed as

$$\mathrm{DI}_{\max} = 6 + 10\log_{10}\sqrt{1+4Q^2} \ \mathrm{dB} \approx 9 + 10\log_{10}Q \ \mathrm{dB} \tag{69}$$

For $a_1 = 1.105$, $Q = 10$ and the maximum directivity index is 19 dB which is a 6 dB improvement over that of the first-degree discriminating function of Eq. (30). In the example presented in this section, $a_1 = 1.105, a_2 = 1.200, \mathrm{DI}_{\max} = 17.8$ dB. As a_2 moves closer to a_1, the maximum directivity index will move closer to 19 dB. For a specified a_1, Eq. (69) represents an upper bound on the maximum directivity index, the bound approached more closely as a_2 moves more closely to a_1.

3.3 Design of discriminating functions from the magnitude response of digital filters

In designing and implementing transfer functions of IIR digital filters, advantage has been taken of the wealth of knowledge and practical experience accumulated in the design and implementation of the transfer functions of analog filters. Continuous-time transfer functions are, by means of the bilinear or impulse-invariant transformations, transformed into equivalent discrete-time transfer functions. The goal of this section is to do a similar thing by generating discriminating functions from the magnitude response of digital filters. As a starting point, consider the following frequency response:

$$H\left(e^{j\omega}\right) = \frac{1-\rho}{1-\rho e^{-j\omega}} \tag{70}$$

where ρ is real, positive and less than 1. Equation (70) corresponds to a causal, stable discrete-time system. The digital frequency ω is not to be confused with the analog frequency ω appearing in previous sections. The magnitude-squared response of this system is obtained from Eq. (70) as

$$\left|H\left(e^{j\omega}\right)\right|^2 = \frac{1-2\rho+\rho^2}{1-2\rho\cos\omega+\rho^2} \tag{71}$$

Letting $\rho = e^{-\sigma}$ allows one to recast Eq. (71) into the simpler form

$$\left|H\left(e^{j\omega}\right)\right|^2 = \frac{\cosh\sigma - 1}{\cosh\sigma - \cos\omega} \tag{72}$$

If the variable ω is replaced by ψ, the resulting function looks like the discriminating function of Eq. (30) where $a = \cosh\sigma$. This suggests a means for generating discriminating functions from the magnitude response of digital filters. Express the magnitude-squared response of the filter in terms of $\cos\omega$ and define

$$g_{u_L}(\psi) \triangleq \left| H\left(e^{j\psi}\right) \right|^2 \tag{73}$$

To illustrate the process, consider the magnitude-squared response of a low pass Butterworth filter of order 2, which has the magnitude-squared function

$$\left| H\left(e^{j\omega}\right) \right|^2 = \frac{1}{1 + \left[\dfrac{\tan(\omega/2)}{\tan(\omega_c/2)} \right]^4} \tag{74}$$

where ω_c is the cutoff frequency of the filter. Utilizing the relationship

$$\tan^2\left(\frac{A}{2}\right) = \frac{1 - \cos A}{1 + \cos A} \tag{75}$$

one can express Eq. (74) as

$$\left| H\left(e^{j\omega}\right) \right|^2 = \frac{\alpha(1 + \cos\omega)^2}{\alpha(1 + \cos\omega)^2 + (1 - \cos\omega)^2} \tag{76}$$

where

$$\alpha = \tan^4\left(\frac{\omega_c}{2}\right) = \frac{(1 - \cos\omega_c)^2}{(1 + \cos\omega_c)^2} \tag{77}$$

The substitution of Eq. (77) into Eq. (76) and simplifying yields the final result

$$\left| H\left(e^{j\omega}\right) \right|^2 = \frac{1 - \cos\theta}{2} \frac{1 + 2\cos\omega + \cos^2\omega}{1 - 2\cos\theta\cos\omega + \cos^2\omega} \tag{78}$$

where

$$\cos\theta = \frac{2\cos\omega_c}{1 + \cos^2\omega_c} \tag{79}$$

By replacing ω by ψ in Eq. (78), one obtains the discriminating function

$$g_{u_L}(\psi) = \frac{1 - \cos\theta}{2} \frac{1 + 2\cos\psi + \cos^2\psi}{1 - 2\cos\theta\cos\psi + \cos^2\psi} \tag{80}$$

where ω_c is replaced by ψ_c in Eq. (79). A plot of Eq. (80) is shown in Fig. 3 for $\psi_c = 10°$. From the figure it is observed that $\psi_c = 10°$ is the 6-dB down angle because the

discriminating function is equal to the magnitude-squared function of the Butterworth filter. The discriminating function of Fig. 3 can be said to be providing a "maximally-flat beam" of order 2 in the look direction u_L. Equation (80) cannot be realized by a parallel interconnection of first-order prototype filters because the roots of the denominator of Eq. (80) are complex. Its realization requires the development of a second-order prototype filter which is the focus of current research.

4. Summary and future research

4.1 Summary

The objective of this paper is to improve the directivity index, beamwidth, and the flexibility of spatial filters by introducing spatial filters having rational discriminating functions. A first-order prototype filter has been presented which has a rational discriminating function of degree one. By interconnecting prototype filters in parallel, a rational discriminating function can be created which has real distinct simple poles. As brought out by Eq. (33), a negative aspect of the prototype filter is the appearance at the output of a spurious frequency whose value is equal to the input frequency divided by the parameter a of the filter where $a > 1$. Since the directivity of the filter is inversely proportional to $a-1$, there exists a tension as a approaches 1 between an arbitrarily increasing directivity D and destructive interference between the real and spurious frequencies. The problem was
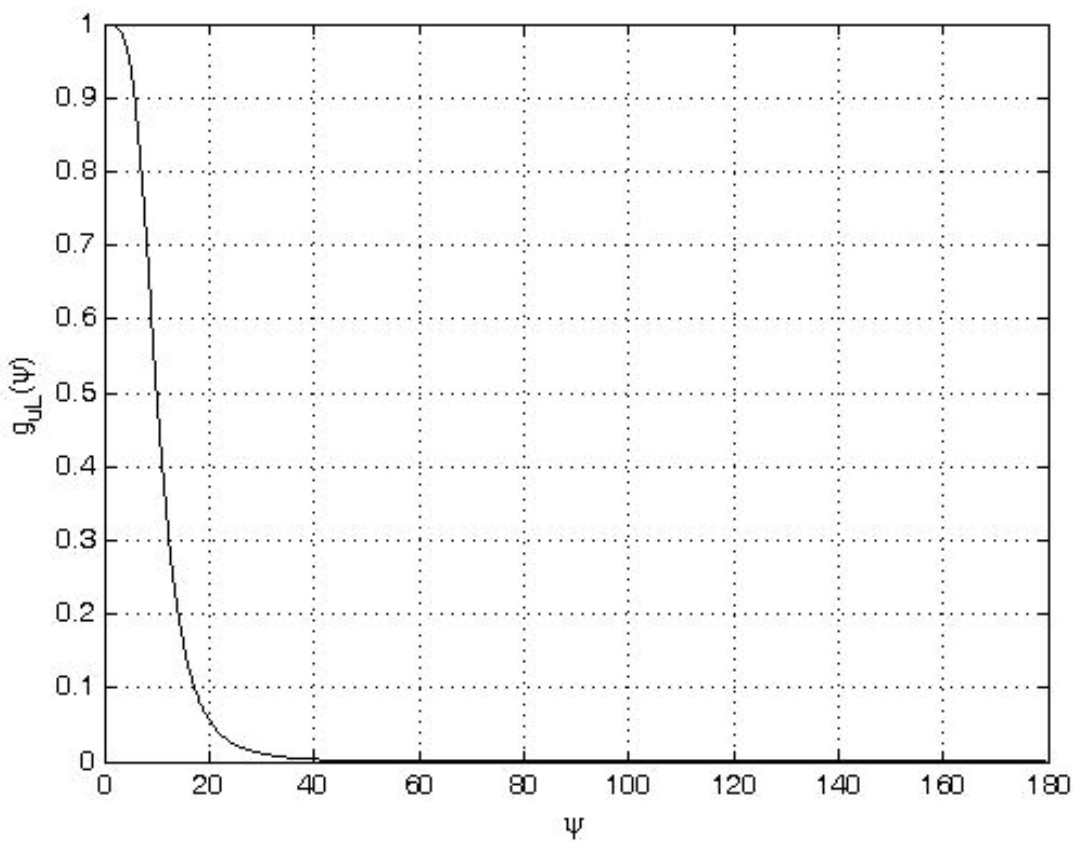

Fig. 3. Discriminating function of Eq. (80).

alleviated by placing a temporal bandpass filter at the output of the prototype filter and assigning *a* the value equal to the ratio of the upper to the lower cutoff frequencies of the bandpass filter. This resulted in the dependence of the directivity index DI on the value of the bandpass filter's quality factor Q as indicated by Eqs. (42) and (43). Consequently, for the prototype filter to be useful, the input plane wave function must be a bandpass signal which fits within the pass band of the temporal bandpass filter. It was noted in Section 2.3 that for $Q = 10$ the directivity index is 13 dB and the beamwidth is 33.9º. Directional acoustic sensors as they exist today have discriminating functions that are polynomials. Their processors do not have the spurious frequency problem. The vector sensor has a maximum directivity index of 6.02 dB and the associated beamwidth is 104.9º. According to Eq. (42) the prototype filter has a DI of 6.02 dB when $Q = 1.94$. The corresponding beamwidth is 87.3º. Section 3.2 demonstrated that the directivity index and the beamwidth can be improved by adding an additional pole. Figure 4 illustrates the directivity index and the beamwidth for the case of two equal roots or poles in the denominator of the discriminating function. As a means of comparison, it is instructive to consider the dyadic sensor which has a polynomial of the second degree as its discriminating function. The sensor's maximum directivity index is 9.54 dB and the associated beamwidth is 65º. The directivity index in Fig. 4 varies from 9.5 dB at $Q = 1$ to 19.0 dB at $Q = 10$. The beamwidth varies from 63.2° at $Q = 1$ to 19.7° at $Q = 10$. The directivity index and beamwidth of the two-equal-poles discriminating function at $Q = 1$ is essentially the same as that of the dyadic sensor. But as the quality factor increases, the directivity index goes up while the beamwidth goes down. It is important to note that the curves in Fig. 4 are theoretical curves. In any practical implementation, one may be required to operate at the lower end of each curve. However, the performance will still be an improvement over that of a dyadic sensor. The two-equal-poles case cannot be realized exactly by first-order prototype filters, but the implementation presented in Section 3.2 comes arbitrarily close. Finally, in Section 3.3 it was shown that discriminating functions can be derived from the magnitude-squared response of digital filters. This allows a great deal of flexibility in the design of discriminating functions. For example, Section 3.3 used the magnitude-response of a second-order Butterworth digital filter to generate a discriminating function that provides a "maximally-flat beam" centered in the look direction. The beamwidth is controlled directly by a single parameter.

4.2 Future research

Many rational discriminating functions, specifically those with complex-valued poles and multiple-order poles, cannot be realized as parallel interconnections of first-order prototype filters. Examples of such discriminating functions appear in Figs. 2 and 3. Research is underway involving the development of a second-order temporal-spatial filter having the prototypical beampattern

$$B\left(\omega : \psi\right) = \frac{g_{u_L}\left(\psi\right)}{\left(j\omega\right)^2} \tag{81}$$

where the prototypical discriminating function $g_{u_L}\left(\psi\right)$ has the form

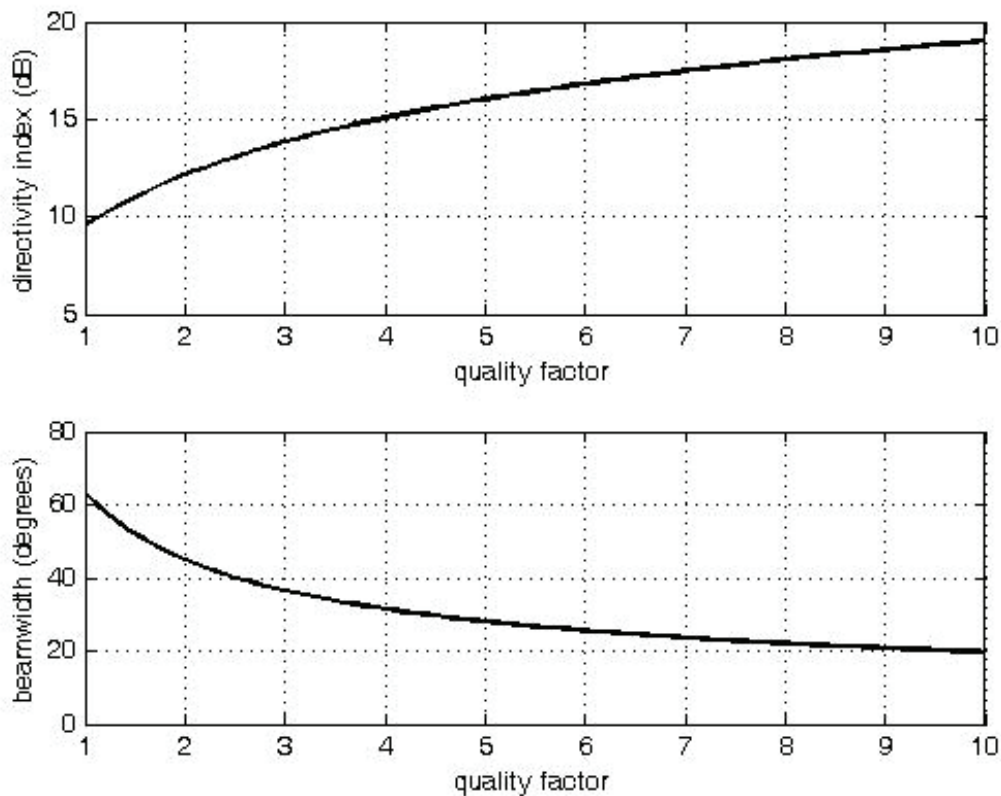$$g_{u_L}\left(\psi\right) = \frac{d_0 + d_1 \cos\psi}{1 + c_1 \cos\psi + c_2 \cos^2\psi} \tag{82}$$

Fig. 4. DI and beamwidth as a function of Q.

With the second-order prototype in place, the discriminating function of Eq. (80), as an example, can be realized by expressing it as a partial fraction expansion and connecting in parallel two prototypal filters. For the first, $d_0 = (1 - \cos\theta)/2$ and $d_1 = c_1 = c_2 = 0$, and for the second, $d_0 = 0, d_1 = \sin^2\theta, c_1 = -2\cos\theta, c_2 = 1$. Though the development of a second-order prototype is critical for the implementation of a more general rational discriminating function than that of the first-order prototype, additional research is necessary for the first-order prototype. In Section 2.2 the number of spatial dimensions was reduced from three to one by restricting pressure measurements to a radial line extending from the origin in the direction defined by the unit vector u_L. This allowed processing of the plane-wave pressure function by a temporal-spatial filter describable by a linear first-order partial differential equation in two variables (Eq. (21)). The radial line (when finite in length) represents a linear aperture or antenna. In many instances, the linear aperture is replaced by a linear array of pressure sensors. This necessitates the numerical integration of the partial differential equation in order to come up with the output of the associated filter. Numerical integration techniques for PDE's generally fall into two categories, finite-difference methods (LeVeque, 2007) and finite-element methods (Johnson, 2009). If q prototypal filters are connected in parallel, the associated set of partial differential equations form a set of q symmetric hyperbolic systems (Bilbao, 2004). Such systems can be numerically integrated using principles of multidimensional wave digital filters (Fettweis and Nitsche, 1991a, 1991b). The resulting algorithms inherit all the good properties known to hold for wave digital filters,

specifically the full range of robustness properties typical for these filters (Fettweis, 1990). Of special interest in the filter implementation process is the length of the aperture. The goal is to achieve a particular directivity index and beamwidth with the smallest possible aperture length. Another important area for future research is studying the effect of noise (both ambient and system noise) on the filtering process. The fact that the prototypal filter tends to act as an integrator should help soften the effect of uncorrelated input noise to the filter. Finally, upcoming research will also include the array gain (Burdic, 1991) of the filter prototype for the case of anisotropic noise (Buckingham, 1979a,b; Cox, 1973). This paper considered the directivity index which is the array gain for the case of isotropic noise.

5. References

Bienvenu, G. & Kopp, L. (1980). Adaptivity to background noise spatial coherence for high resolution passive methods, *Int. Conf. on Acoust., Speech and Signal Processing*, pp. 307-310.

Bilbao, S. (2004). *Wave and Scattering Methods for Numerical Simulation*, John Wiley and Sons, ISBN 0-470-87017-6, West Sussex, England.

Bresler, Y. & Macovski, A. (1986). Exact maximum likelihood parameter estimation of superimposed exponential signals in noise, *IEEE Trans. ASSP*, Vol. ASSP-34, No. 5, pp. 1361-1375.

Buckingham, M. J. (1979a). Array gain of a broadside vertical line array in shallow water, *J. Acoust. Soc. Am.*, Vol. 65, No. 1, pp. 148-161.

Buckingham, M. J. (1979b). On the response of steered vertical line arrays to anisotropic noise, *Proc. R. Soc. Lond. A*, Vol. 367, pp. 539-547.

Burdic, W. S. (1991). *Underwater Acoustic System Analysis*, Prentice-Hall, ISBN 0-13-947607-5, Englewood Cliffs, New Jersey, USA.

Cox, H. (1973). Spatial correlation in arbitrary noise fields with application to ambient sea noise, *J. Acoust. Soc. Am.*, Vol. 54, No. 5, pp. 1289-1301.

Cray, B. A. (2001). Directional acoustic receivers: signal and noise characteristics, *Proc. of the Workshop of Directional Acoustic Sensors*, Newport, RI.

Cray, B. A. (2002). Directional point receivers: the sound and the theory, *Oceans '02*, pp. 1903-1905.

Cray, B. A.; Evora, V. M. & Nuttall, A. H. (2003). Highly directional acoustic receivers, *J. Acoust. Soc. Am.*, Vol. 13, No. 3, pp. 1526-1532.

D'Spain, G. L.; Hodgkiss, W. S.; Edmonds, G. L.; Nickles, J. C.; Fisher, F. H.; & Harris, R. A. (1992). Initial analysis of the data from the vertical DIFAR array, *Proc. Mast. Oceans Tech. (Oceans '92)*, pp. 346-351.

D'Spain, G. L.; Luby, J. C.; Wilson, G. R. & Gramann R. A. (2006). Vector sensors and vector sensor line arrays: comments on optimal array gain and detection, *J. Acoust. Soc. Am.*, Vol. 120, No. 1, pp. 171-185.

Fettweis, A. (1990). On assessing robustness of recursive digital filters, *European Transactions on Telecommunications*, Vol. 1, pp. 103-109.

Fettweis, A. & Nitsche, G. (1991a). Numerical Integration of partial differential equations using principles of multidimensional wave digital filters, *Journal of VLSI Signal Processing*, Vol. 3, pp. 7-24, Kluwer Academic Publishers, Boston.

Fettweis, A. & Nitsche, G. (1991b). Transformation approach to numerically integrating PDEs by means of WDF principles, *Multidimensional Systems and Signal Processing*, Vol. 2, pp. 127-159, Kluwer Academic Publishers, Boston.

Hawkes, M. & Nehorai, A. (1998). Acoustic vector-sensor beamforming and capon direction estimation, *IEEE Trans. Signal Processing*, Vol. 46, No. 9, pp. 2291-2304.

Hawkes, M. & Nehorai, A. (2000). Acoustic vector-sensor processing in the presence of a reflecting boundary, *IEEE Trans. Signal Processing*, Vol. 48, No. 11, pp. 2981-2993.

Hines, P. C. & Hutt, D. L. (1999). SIREM: an instrument to evaluate superdirective and intensity receiver arrays, *Oceans 1999*, pp. 1376-1380.

Hines, P. C.; Rosenfeld, A. L.; Maranda, B. H. & Hutt, D. L. (2000). Evaluation of the endfire response of a superdirective line array in simulated ambient noise environments, *Proc. Oceans 2000*, pp. 1489-1494.

Johnson, C. (2009). *Numerical Solution of Partial Differential Equations by the Finite-Element Method*, Dover Publications, ISBN-13 978-0-486-46900-3, Mineola, New York, USA

Krim, H. & Viberg, M. (1996). Two decades of array signal processing research, *IEEE Signal Processing Magazine*, Vol. 13, No. 4, pp. 67-94.

Kumaresan, R. & Shaw, A. K. (1985). High resolution bearing estimation without eigendecomposition , *Proc. IEEE ICASSP 85*, p. 576-579, Tampa, FL.

Kythe, P. K.; Puri, P. & Schaferkotter, M. R. (2003). *Partial Differential Equations and Boundary Value Problems with Mathematica*, Chapman & Hall/ CRC, ISBN 1-58488-314-6, Boca Raton, London, New York, Washington, D.C.

LeVeque, R. J. (2007). *Finite Difference Methods for Ordinary and Partial Differential Equations*, SIAM, ISBN 978-0-898716-29-0, Philadelphia, USA.

Nehorai, A. & Paldi, E. (1994). Acoustic vector-sensor array processing, *IEEE Trans. Signal Processing*, Vol. 42, No. 9, pp. 2481-2491.

Schmidlin, D. J. (2007). Directionality of generalized acoustic sensors of arbitrary order, *J. Acoust. Soc. Am.*, Vol. 121, No. 6, pp. 3569-3578.

Schmidlin, D. J. (2010a). Distribution theory approach to implementing directional acoustic sensors, *J. Acoust. Soc. Am.*, Vol. 127, No. 1, pp. 292-299.

Schmidlin, D. J. (2010b). Concerning the null contours of vector sensors, *Proc. Meetings on Acoustics*, Vol. 9, Acoustical Society of America.

Schmidlin, D. J. (2010c). The directivity index of discriminating functions, *Technical Report No. 31-2010-1*, El Roi Analytical Services, Valdese, North Carolina.

Schmidt, R. O. (1986). Multiple emitter location and signal parameter estimation, *IEEE Trans. Antennas and Propagation*, Vol. AP-34, No. 3, pp. 276-280.

Silvia, M. T. (2001). A theoretical and experimental investigation of acoustic dyadic sensors, *SITTEL Technical Report No. TP-4*, SITTEL Corporation, Ojai, Ca.

Silvia, M. T.; Franklin, R. E. & Schmidlin, D. J. (2001). Signal processing considerations for a general class of directional acoustic sensors, *Proc. of the Workshop of Directional Acoustic Sensors*, Newport, RI.

Van Veen, B. D. & Buckley, K. M. (1988). Beamforming: a versatile approach to spatial filtering, *IEEE ASSP Magazine*, Vol. 5, No. 2, pp. 4-24.

Wong, K. T. & Zoltowski, M. D. (1999). Root-MUSIC-based azimuth-elevation angle-of-arrival estimation with uniformly spaced but arbitrarily oriented velocity hydrophones, *IEEE Trans. Signal Processing*, Vol. 47, No. 12, pp. 3250-3260.

Wong, K. T. & Zoltowski, M. D. (2000). Self-initiating MUSIC-based direction finding in underwater acoustic particle velocity-field beamspace, *IEEE Journal of Oceanic Engineering*, Vol. 25, No. 2, pp. 262-273.

Wong, K. T. & Chi, H. (2002). Beam patterns of an underwater acoustic vector hydrophone located away from any reflecting boundary, *IEEE Journal Oceanic Engineering*, Vol. 27, No. 3, pp. 628-637.

Ziomek, L. J. (1995). *Fundamentals of Acoustic Field Theory and Space-Time Signal Processing*, CRC Press, ISBN 0-8493-9455-4, Boca Raton, Ann Arbor, London, Tokyo.

Zou, N. & Nehorai, A. (2009). Circular acoustic vector-sensor array for mode beamforming, *IEEE Trans. Signal Processing*, Vol. 57, No. 8, pp. 3041-3052.

Advances in Sound Localization

Edited by Dr. Pawel Strumillo

Sound source localization is an important research field that has attracted researchers' efforts from many technical and biomedical sciences. Sound source localization (SSL) is defined as the determination of the direction from a receiver, but also includes the distance from it. Because of the wave nature of sound propagation, phenomena such as refraction, diffraction, diffusion, reflection, reverberation and interference occur. The wide spectrum of sound frequencies that range from infrasounds through acoustic sounds to ultrasounds, also introduces difficulties, as different spectrum components have different penetration properties through the medium. Consequently, SSL is a complex computation problem and development of robust sound localization techniques calls for different approaches, including multisensor schemes, null-steering beamforming and time-difference arrival techniques. The book offers a rich source of valuable material on advances on SSL techniques and their applications that should appeal to researches representing diverse engineering and scientific disciplines.

How to reference

In order to correctly reference this scholarly work, feel free to copy and paste the following:

Dean Schmidlin (2011). Direction-Selective Filters for Sound Localization, Advances in Sound Localization, Dr. Pawel Strumillo (Ed.), ISBN: 978-953-307-224-1, InTech, Available from: http://www.intechopen.com/books/advances-in-sound-localization/direction-selective-filters-for-sound-localization

INTECH
open science | open minds